

SOME RECENT RESULTS IN TOMOGRAPHY

Yoram Bresler

Coordinated Science Laboratory
Department of Electrical and Computer Engineering
University of Illinois at Urbana-Champaign
1308 W. Main St. · Urbana, IL 61801

ABSTRACT

We present an overview of two recent developments in tomography: design of optimum scan patterns for time-varying objects; and an efficient iterative edge-preserving algorithm for limited-angle data. The first development involves the introduction of a new problem definition and changing the "rules of the game" by unconventional acquisition formats. It also employs the mathematical tools of lattice theory, which have seen relatively little use in this area. The second development, on the other hand, addresses a classical and long standing problem, by a combination of more rigorous analysis and modeling with some heuristic twists.

1. INTRODUCTION

We present an overview of two recent developments in tomography: (i) Design of optimum scan patterns for time-varying tomography [1, 2]; and (ii) Efficient iterative limited-angle tomographic reconstruction using non-linear constraints [3].

In the first problem, we consider the tomography of objects with spatially localized temporal variation, such as a thorax cross-section with a beating heart, or an internal organ with contrast agent flowing through it. The conventional scan format, in which projections are taken progressively around the object, requires high, and sometimes infeasible scan rates to avoid motion artifacts in the reconstructed images. We formulate the problem of data acquisition as a time-sequential sampling problem of spatially and temporally bandlimited signals, where only one view can be taken at a time, but the time interval between successive views is independent of their angular separation. These conditions, naturally satisfied in magnetic resonance imaging and in x-ray CT using electronic beam deflection, can also be satisfied by a conventional system with a continuously

and rapidly spinning gantry with source pulsing. Theoretical analysis, which includes tight performance bounds, shows that by using an optimally scrambled angular sampling order, the required scan rate can be lowered as much as four times, while preserving image quality. The analysis also greatly simplifies the design of the optimum scan pattern by reducing it to a constrained geometric packing problem. The resulting design procedure depends only on pre-specified geometric and spectral parameters, and the desired spatial resolution. The resulting patterns have a simple congruential structure. Reconstruction is accomplished by interpolation (at a negligible computational cost) to standard time-invariant scan format, followed by conventional reconstruction.

Previous attempts for limited angle reconstruction [4]-[6] have achieved only limited success: they either used too mild constraints that were insufficient to adequately regularize the severely ill-posed problem, or highly structured prior knowledge, which limited the applicability of the method to very specialized scenarios. In addition, many of these algorithms involved iterative back-projection-reprojection, requiring intensive computation. These same steps also often involved idealized modeling that ignored the discrete nature of practical data, further degrading the results.

In this paper we describe our recent work [3] that addresses the foregoing problems. We report on a new, efficient iterative algorithm for reconstructing piecewise-smooth images with sharp edges from a finite number of parallel-ray projections collected over a limited angular range. Edge-preserving regularization has been used successfully to regularize other ill-posed problems, such as surface reconstruction, image flow, and even noisy full-angle tomography (cf. [7]-[10]). However, to date, with the exception of [11], these algorithms, which typically require a great deal of computation, have not been applied to the limited-angle problem.

Our approach to the efficient minimization of the resulting cost functional has two components. The first is a new, accurate and efficient FFT-based algorithm to implement the conjugate gradient iteration for this problem

This work was supported in part by National Science Foundation grant No. MIP 91-57377 and Joint Services Electronic Program, Grant No. N00014-90-J-1270

[12]. In contrast to previous transform-domain iterative algorithms [13], this algorithm is based on rigorous modeling of the discrete projections, resulting in improved accuracy. The second component of our approach [3], for nonconvex regularization functionals, is a new deterministic relaxation algorithm that solves a sequence of convex optimization problems, each of which is solved by the original conjugate gradient algorithm. Reconstructions using synthetic data demonstrate the effectiveness of this approach.

2. OPTIMAL SCAN DESIGN FOR TIME-VARYING TOMOGRAPHIC IMAGING

We consider a class \mathcal{F} of time-varying images $\mu(x, y, t)$ of radius R_m with rapid temporal variation bandlimited to b_t , which is spatially localized to a circular region of radius r_m , and slower unlocalized variation bandlimited to $B_t < b_t$. Such images arise e.g., in cross-sectional cardiac imaging, where rapid variation is restricted to the heart, with superimposed unlocalized slower variation, e.g., due to breathing. We consider the reconstruction of $\mu(x, y, t)$ from its parallel-beam projections $\tilde{\mu}(\rho, \phi, t)$. We assume continuous acquisition in the radial variable ρ , since its sampling can be made fine enough to neglect. The *sampling schedule* given by the set $\Psi \triangleq \{(\phi_l, lT)\}_{l=-\infty}^{\infty}$ specifies the angle and time instant of successive projections, and therefore completely defines the acquisition procedure. In particular, we denote by $\Omega(B_\rho)$ the set of B_ρ -reconstructive schedules consisting of those TS sampling schedules Ψ for which an exact reconstruction $\hat{\mu}(x, y, t)$ of $\mu(x, y, t)$ bandlimited to a spatial bandwidth B_ρ is possible (for all t) from the samples on Ψ of $\tilde{\mu}(\rho, \phi, t)$. Our goal is to design such a schedule that will maximize the inter-projection time interval T .

To simplify the problem (at a negligible loss in achievable performance [1]), we only consider the subset $\Gamma(B_\rho) \subset \Omega(B_\rho)$ of TS sampling schedules that lie on a *lattice* in the (ϕ, t) plane. We denote by Λ_A and Λ_A^* a lattice and its polar lattice, defined by the basis matrices A and $A^* \triangleq A^{-T}$, respectively. A lattice Λ_A is said to *pack* a given set $\mathcal{L} \subset \mathbb{R}^2$, if replicas (aliases) of \mathcal{L} centered on the points of Λ_A do not overlap. We denote by $\mathcal{P}(\mathcal{L})$ the set of all lattices that pack \mathcal{L} . Now, an analysis of the 3-D Fourier transform $\tilde{M}(u_\rho, u_\phi, u_t)$ of the projections $\tilde{\mu}(\rho, \phi, t)$ of objects in the class \mathcal{F} reveals that they have an odd shaped support. The condition for alias-free reconstruction from samples on a lattice Λ_A involves the packing, in 2-D, of a cross-shaped spectral support \mathcal{B} by the polar lattice Λ_A^* . In turn, the dimensions of \mathcal{B} are determined by the geometric and spectral parameters R_m, r_m, b_t, B_t of the object class \mathcal{F} , and by the desired reconstruction bandwidth (resolution) B_ρ .

With these preliminaries we have the following results [1]: A lattice Λ_A is a B_ρ -reconstructive TS schedule, i.e., $\Lambda_A \in$

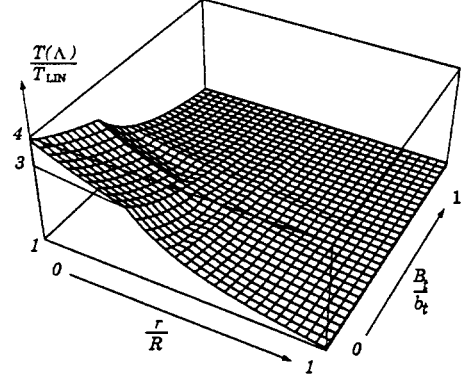


Figure 1: upper bound on figure of merit

$\Gamma(B_\rho)$, if and only if $\Lambda_A^* \in \mathcal{P}(\mathcal{B})$ and has the basis

$$A^* = \begin{bmatrix} \frac{p}{\pi} & \frac{l}{\pi} \\ u_1 & u_2 \end{bmatrix}, \quad p, l \in \mathbb{Z}, \quad \gcd(p, l) = 1, \quad \frac{u_1}{u_2} \in \mathcal{Q}, \quad (1)$$

where p and l are coprime and u_1/u_2 is a rational number. A similar result, but with A^* having one less degree of freedom, applies when the number K of distinct projection angles is set a priori, e.g., owing to constraints on detectors. (In our simulation, $K = 256$). In all cases, the inter-projection time interval is

$$T = T(\Lambda_A, \mathcal{B}) = \det(A)/\pi. \quad (2)$$

It follows that the scan optimization problem is reduced to

$$\Lambda_{\text{optimum}} = \arg \max_{\Lambda \in \Gamma(B_\rho)} T(\Lambda) = \arg \min_{\substack{\Lambda_A^* \in \mathcal{P}(\mathcal{B}) \\ A^* \in \mathcal{C}}} \det[A^*] \quad (3)$$

where \mathcal{C} represents the set of matrices satisfying the constraint (1). This is a purely geometric problem: find the polar lattice Λ_A^* that packs the spectral support \mathcal{B} the tightest possible, subject to the constraint (1). The optimum lattice Λ_{optimum} (and hence, the schedule Ψ) is then determined by $A = (A^*)^{-T}$, and the optimum inter-projection time interval is computed via (2). A simple procedure for this geometrical design, starting by relaxing the constraints (1) to first find the critical packing of \mathcal{B} , and then minimally modifying the lattice to satisfy the constraints is proposed in [2].

Using this result, we derived an (essentially) achievable upper bound on the possible relative improvement $\frac{T(\Lambda)}{T_{LIN}}$ of the sampling lattice Λ over a conventional linear progressive scan Λ_{LIN} . This bound (plotted in Fig. 1) can be used to judge the merit of performing the optimization, and as a stopping criterion in the optimization procedure itself. We see the greatest improvements when $\frac{r_m}{R_m}$ and $\frac{B_t}{b_t}$ are both less than $\frac{1}{3}$, i.e., when temporal variation is spatially concentrated by greater than a factor of three within the

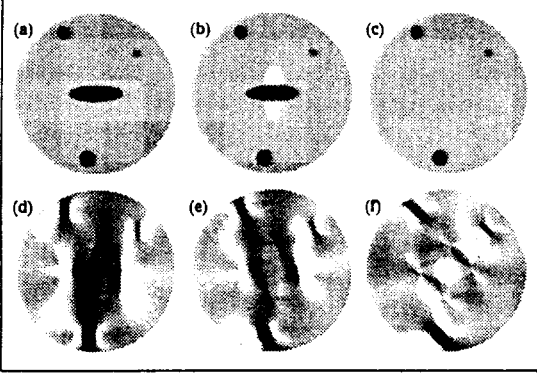


Figure 2: Reconstructions with $T = 1/64$. (a)-(c) optimal sampling (d)-(f) linear sampling

center region, and it is at least three times greater there than in the periphery.

Numerical results In the simulations 40 cycles of $K = 256$ projections each are synthesized (i.e., “measured”) according to the specified sampling schedule. To reconstruct, we interpolate these projections via low-pass filtering in the (u_t, u_ϕ) plane over the modeled spectral support \mathcal{B} , producing a complete set of 256 projections at specific output times. The data are then reconstructed using a standard FBP algorithm, with a Hamming weighted ρ -filter of bandwidth B_ρ .

Figs. 2(a)-(c) show artifact-free reconstructions of a phantom, at times $t = 0$, $t = 0.5$ and $t = 1$, respectively, using the optimized schedule, for a somewhat reduced spatial bandwidth, with $T = 1/64$. This intersample interval is four times larger than allowed for alias-free reconstruction from a conventional linear progressive scan. The time-varying component of the phantom consists of two perpendicular centered ellipses, A and B , whose densities are temporally modulated by the sinc functions $\text{sinc } \pi t$ and $\text{sinc } \pi(t - 2)$, respectively. For this phantom $\frac{r_m}{R_m} = \frac{1}{3}$, $R_m = 1$, $b_t = 0.5$ and $B_t = 0$. The same intersample interval $T = 1/64$ leads to useless reconstructions from a conventional linear scan (Figs. 2(d)-(f)). Reconstructions with an optimized schedule of images that are only approximately bandlimited show similar improvements [2].

3. EDGE-PRESERVING REGULARIZATION FOR LIMITED-ANGLE TOMOGRAPHY

Our goal is to reconstruct an estimate $\hat{f} \in L^2(R^2)$ of the object $f \in L^2(R^2)$ from a set $g_D \in \{\ell^2(Z)\}^P$ of noisy, sampled, bandlimited parallel-ray projections of f collected at P arbitrary view angles. We represent \hat{f} by a discrete image $\hat{f}_D \in R^{N \times N}$: the coefficients of its expansion in a basis of translates of a single given generating function $b \in$

$L^2(R^2)$. The projections are then modeled as $g_D \approx \mathcal{A}\hat{f}_D$, where $\mathcal{A} : R^{N \times N} \rightarrow \{\ell^2(Z)\}^P$ is the discrete-continuous-discrete projection operator that depends on b and on the particular projection geometry being used [12]. We define \hat{f}_D as a solution to the following optimization problem:

$$\min_{\hat{f}_D} \left\{ \frac{1}{2} \|g_D - \mathcal{A}\hat{f}_D\|_{\mathcal{W}}^2 + \lambda_A \mathcal{C}_A \hat{f}_D + \lambda_E \mathcal{C}_E \hat{f}_D \right\}, \quad (4)$$

where $\lambda_i \in R$, $i = A, E$ are regularization parameters, and $\|\cdot\|_{\mathcal{W}}$ is a weighted 2-norm. The regularization functional \mathcal{C}_A penalizes image values exceeding preset minimum and maximum values (e.g, zero, and the minimum of all ray-sums going through given point, respectively). \mathcal{C}_E encourages the formation of images consisting of piecewise-smooth regions with sharp boundaries.

\mathcal{C}_E is given by

$$\mathcal{C}_E \hat{f}_D = \sum_{m \in Z_N^2} \sum_{i=x,y} \phi[\mathcal{D}_i \hat{f}_D(m)], \quad (5)$$

where $Z_N^2 = \{1, \dots, N\}^2$, $\mathcal{D}_i : R^{N \times N} \rightarrow R^{N \times N}$, $i = x, y$ are the horizontal and vertical sampled-derivative operators, respectively, and ϕ is a positive, symmetric function usually referred to as the *neighborhood interaction function* or the *influence function* [9, 7, 8]. Although a convex ϕ is recommended on various theoretical grounds [10], our numerical results show that in this application a nonconvex ϕ , e.g $\phi_E(t) = t^2[1 - (t/T_E)^3]^{-1}$, produced consistently superior results.

To facilitate optimization in the case of non-convex ϕ , we convert (4) into a sequence of convex optimization problems. At the k -th step, \mathcal{C}_E is replaced by \mathcal{C}_E^k , defined by

$$\mathcal{C}_E^k \hat{f}_D = \sum_{m \in Z_N^2} \sum_{i=x,y} e_i^{k-1}(m) [\mathcal{D}_i \hat{f}_D(m)]^2. \quad (6)$$

Denoting by \hat{f}_D^k the solution to the k -th such convex optimization problem, e_i^{k-1} , $i = x, y$ are vertical and horizontal edge maps found from \hat{f}_D^{k-1} :

$$e_i^k(m, n) = \rho(\mathcal{H}^k \mathcal{D}_i \hat{f}_D^k(m, n)) \quad i = x, y \quad (7)$$

where \mathcal{H}^k is a sequence of blurring operators with monotone decreasing blur converging to the identity operator, and $\rho(t)$ is a positive symmetric decreasing function. The motivation for this algorithm, is that $e_i(m_x, m_y)$, which takes on lower values at edge locations (as determined from the previous iteration) prevents smoothing across edges. The role of the blur \mathcal{H}^k is to account for the imperfect localization of the edges in intermediate stages of the algorithm. We can prove that with the choice $\rho(t) = \phi(t)/t^2$ this iterative algorithm converges to a local minimum of the original criterion (4). For convex influence functions, this will also be the global minimum.

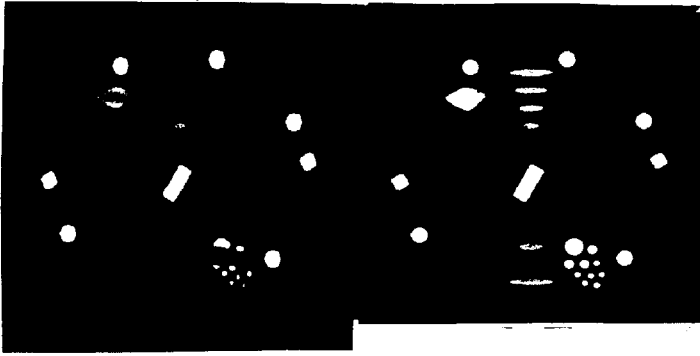


Figure 3: Missing angle (22°) reconstructions. (a) FBP with noiseless data. (b) Iterative algorithm with ϕ_E and APSNR= 40 dB.

We perform the optimization of the k -th convex version of (4) [using (6)] by an efficient conjugate gradient (CG) algorithm described in [12], for which the main step at each iteration is a $2N \times 2N$ 2-D discrete convolution implemented exactly using an FFT.

Charbonnier et al. [14] and Barlaud et al. [15] have used a relaxation algorithm similar to ours for full-angle SPECT reconstructions. The convergence proof of our algorithm was inspired by that in [15]. The major difference between our approach and theirs is that they do not blur what we call the edge maps. (In their derivation of the algorithm, they do not use the idea of an edge map. They also use a different method for solving each convex optimization problem.) However, for limited-angle tomography the initial edge map is usually very unreliable, and we have found that using a blurred edge map is essential when a nonconvex ϕ is to be implemented.

Numerical Experiments We simulate noisy discrete parallel-ray projection data collected by unit-width integrating detectors, over 159 view angles evenly spaced from -79° to 79° . We define the average projection SNR (APSNR) as $10 \log_{10}$ of the ratio of total projection to noise energies. Fig. 3-a shows, for reference, a limited angle 240×240 FBP reconstruction (with a Shepp-Logan filter) of a phantom from noiseless projections. In Fig. 3-b, is shown the essentially perfect reconstruction using our algorithm with the non-convex ϕ_E , from limited angle projections with APSNR of 40 dB. This iterative reconstruction required about 50 iterations or a total of less than three minutes on a Silicon Graphics Indy workstation – about six times as long as the standard FBP algorithm. Detailed qualitative and quantitative comparisons between several influence functions, and studies of the effects of missing angle, number of views, and their angular distribution are reported in [3]. (See also [12] for a similar scenario with the Huber influence function).

4. REFERENCES

- [1] N. P. Willis and Y. Bresler, "Optimal scan design for time varying tomographic imaging I: Theoretical analysis and fundamental limitations", to appear in *IEEE Trans. Image Processing*, May 1995.
- [2] N. P. Willis and Y. Bresler, "Optimal scan design for time varying tomographic imaging II: Efficient design and experimental validation", to appear in *IEEE Trans. Image Processing*, May 1995.
- [3] A. H. Delaney and Y. Bresler, "Edge preserving regularization for limited angle tomography", submitted to *IEEE Trans. Image Processing*, 1994.
- [4] R. Rangayyan, A. P. Dhawan, and R. Gordan, "Algorithms for limited-view computed tomography: an annotated bibliography and a challenge," *Applied Optics*, vol. 24, no. 23, pp. 4000–4012, 1985.
- [5] D. Verhoeven, "Limited-data computed tomography algorithms for the physical sciences," *Applied Optics*, vol. 32, no. 20, pp. 3736–3754, 1993.
- [6] P. Oskoui and H. Stark, "A comparative study of three reconstruction methods for a limited-view computer tomography problem," *IEEE Trans. Med. Imaging*, vol. 8, no. 1, pp. 43–49, 1989.
- [7] P. J. Green, "Bayesian reconstructions from emission tomography data using a modified EM algorithm," *IEEE Trans. Med. Imaging*, vol. 9, no. 1, pp. 84–93, 1990.
- [8] K. Lange, "Convergence of EM image reconstruction algorithms with Gibbs smoothing," *IEEE Trans. Med. Imaging*, vol. 9, no. 4, pp. 439–446, 1990.
- [9] D. Geman and G. Reynolds, "Constrained restoration and the recovery of discontinuities," *IEEE Trans. Patt. Anal. Mach. Intell.*, vol. 14, no. 3, pp. 367–383, 1992.
- [10] C. Bouman and K. Sauer, "A generalized Gaussian image model for edge-preserving MAP estimation," *IEEE Trans. Image Proc.*, vol. 2, no. 3, pp. 296–310, 1993.
- [11] I. B. Kerfoot and Y. Bresler, "Mean field and information-theoretic algorithms for direct segmentation of tomographic images", in *Proc. IS&T/SPIE Symp. Electr. Imaging Science and Techn.*, San Jose, CA, Feb. 1993, vol. 1905, pp. 956–963.
- [12] A. H. Delaney and Y. Bresler, "A fast iterative reconstruction algorithm for parallel-beam tomography," in *Proc. ICASSP*, (Detroit, MI), May 1993.
- [13] M. I. Sezan and H. Stark, "Applications of convex projection theory to image recovery in tomography and related areas," in *Image Recovery: Theory and Application* (H. Stark, ed.), ch. 11, pp. 415–462, San Diego: Academic Press, Inc., 1987.
- [14] P. Charbonnier, L. Blanc-Feraud, and M. Barlaud, "An adaptive reconstruction method involving discontinuities," in *Proc. ICASSP*, (Minneapolis, MN), April 1993.
- [15] "Deterministic Edge-preserving regularization in Computed Imaging" Research Report No. 94-01, University of Nice- Sophia Antipolis, 1994.